Two-Photon Excitation Fluorescence Correlation Spectroscopy of Diffusion for Gaussian−Lorentzian Volumes

Michele Marrocco[†]

ENEA, via Anguillarese 301, S. Maria di Galeria, Rome, Italy

Received: November 7, 2007; In Final Form: February 11, 2008

Fluorescence correlation spectroscopy (FCS) is valuable in many scientific domains where diffusion plays a fundamental role. One important experimental realization is based on fluorescence induced by two-photon excitation (TPE). In comparison with one-photon excitation (OPE), TPE-FCS defines better the interrogation volume and the background noise is sensibly reduced. Within this context and for overfilled objective lenses, the three-dimensional Gaussian (3DG) approximation, according to which the spectroscopic interaction is spatially defined by Gaussian profiles only, guarantees a simple analytical data interpretation. By contrast, the volume illuminated by the laser beam focused with partially filled objective lenses follows a Gaussian−Lorentzian (GL) distribution that is taken into account by means of numerical methods only. Here we show that contrary to common belief, the assumption of a GL volume does not hamper analytical treatment of TPE-FCS. Differences and similarities in comparison with the 3DG approximation are discussed.

1. Introduction

In the 35 years since its introduction,[1] fluorescence correlation spectroscopy (FCS) has gained the status of a well-established spectroscopic technique that is used to investigate a wide variety of physical and chemical phenomena summarized in textbooks and reviews.[2−8]

The basics of FCS are rather simple. Very briefly, the spectroscopic strategy begins first with the acquisition of time trajectories of laser-induced fluorescence $F(t)$. Having obtained the average signal $\langle F(t)\rangle$, the fluctuations $\delta F(t) = F(t) - \langle F(t)\rangle$ are then useful to determine the correlation function $G(\tau) = \langle \delta F(t + \tau)\delta F(t)\rangle/\langle F(t)\rangle^2$, whose shape can be decoded to sort out the information about physical and chemical phenomena taking place within the volume confined by the laser beam. The decay of $G(\tau)$ is, indeed, rich in information and its expression depends on the interrogation volume described by the function $\varphi(\mathbf{r})$, that is

$$G(\tau) = \frac{\int\int \varphi(\mathbf{r})\, \psi(\mathbf{r} - \mathbf{r}',\tau)\varphi(\mathbf{r}')\, \mathrm{d}\mathbf{r}\, \mathrm{d}\mathbf{r}'}{(\langle C\rangle \int \varphi(\mathbf{r})\, \mathrm{d}\mathbf{r})^2} \qquad (1)$$

where $\psi(\mathbf{r} - \mathbf{r}',\tau) = \langle \delta C(\mathbf{r},t + \tau)\delta C(\mathbf{r}',t)\rangle$ indicates the fluctuating contribution $\delta C(\mathbf{r},t)$ of particle concentration C with average $\langle C\rangle$.

One of the major achievements of the approach recalled in eq 1 is the understanding of diffusion processes.[1−8] This understanding has a key role in several contexts of primary importance. Some examples include chemical reaction kinetics,[1] transport in tumors,[9] protein dynamics,[10,11] intracellular interactions,[12,13] diagnostics of Alzheimer's disease,[14] dual fluorophore assays,[15] diffusion in nanoscopic structures,[16] diffusion of nanocrystals,[17−19] dynamics of DNA chains,[20] and single molecule detection;[21] many other examples can be found in literature.[2−8] Most of these possible applications have in common that the diffusive nature of FCS is brought out by a well-known correlation function that was calculated more than 30 years ago by Aragón and Pecora under the so-called 3DG approximation.[22] This assumption dictates that the interrogation or observation volume, captured by the microscope objective, is constrained within Guassian profiles along the main three spatial axes and, after some algebra, the solution of eq 1 is

$$G_{3DG}(\tau) = G_{3DG}(0)\frac{1}{1 + \tau/\tau_D}\frac{1}{[1 + (w_0/z_{3DG})^2\tau/\tau_D]^{1/2}} \qquad (2)$$

The approximated correlation function $G_{3DG}(\tau)$ is derived from a Brownian diffusion model (with no compensation for other sources of fluctuation) and is very popular among FCS users. It contains four parameters: the first two being the laser beam waist w_0 and the axial width z_{3DG}, which are intrinsic to the optical setup, whereas the correlation amplitude $G_{3DG}(0)$ and the diffusion time τ_D tie in with the molecule under study. In particular, the amplitude is inversely proportional to the number N_{3DG} of molecules in the interrogation volume V_{3DG}, i.e., $G_{3DG}(0) = 2^{-3/2}/N_{3DG}$ with $N_{3DG} = \langle C\rangle V_{3DG}$. Another inverse proportionality relates the diffusion time to the diffusion constant D, i.e., $\tau_D = w_0^2/(4nD)$ with $n = 1$ for one-photon excitation (OPE) and $n = 2$ for two-photon excitation (TPE).

Although eq 2 is formally identical for OPE and TPE, its reliability is surely weaker for OPE. This is a consequence of the confocal pinhole necessary in OPE to limit the noise from spatial regions that are out of focus,[23] and in this regard, all the measurements based on the 3DG approximation could be easily criticized. On the contrary, the approximation seems to hold well for the interpretation of TPE-FCS measurements,[23,24] where the use of the confocal pinhole is not contemplated but the condition of overfilled microscope objective lenses must be obeyed to obtain diffraction-limited focal spots. For partially filled objective lenses, however, the focal volume is no longer Gaussian in the axial direction (i.e., the direction of the optical axis, here called z-axis). More precisely, while Gaussian distributions still characterize the interrogation volume along radial directions (here called x and y), the axial direction is

[†] E-mail: michele.marrocco@casaccia.enea.it. Tel: 39 06 3048 3345. Fax: 39 06 3048 4811.

10.1021/jp710677z CCC: $40.75
Published on Web 04/02/2008

instead characterized by a Lorentzian distribution.[2,12,25,26] The appearance of this combination of spatial dependences is not new in laser spectroscopy,[2] because the three-dimensional Gaussian−Lorentzian (GL) distribution is recognized as the fundamental mode of laser beams.[2,27,28] However, in marked contrast to the importance of such spatial shape of laser excitation, a rigorous analysis of the associated TPE-FCS correlation function is lacking in literature.

In an attempt to clarify this matter, we will try to conceive an answer to a problem that has long puzzled scientists using FCS for various applications, i.e., the problem of an analytical calculation of the correlation function of molecular diffusion studied by means of TPE fluorescence emitted from GL volumes.[29−31] To put this problem in the right perspective, it must be made clear that the method developed here differs from the companion analysis applied recently to treat GL volumes in the context of OPE-FCS.[32] But, in analogy with that work[32] and the 3DG approximation leading to $G_{3DG}(\tau)$ of eq 2, we will restrict ourselves to considering normal diffusion only (i.e., diffusion with time independent diffusion coefficient).[33]

In general, it is known that TPE-FCS of molecular diffusion within GL volumes is solved by means of numerical methods,[29−31] but these have two main limitations. First of all, they do not provide any physical insight into the expected decay of the correlation function. As a matter of fact, correlation decays are obtained from numerical solutions of an integral whose physical significance is lost in favor of the neutral mathematical necessity for manageable results. Second, the fitting routines, used to extract the relevant parameters from the correlation function, are decidedly less convenient if they have to include for each run the calculation of a numerical integral.

In this work, the flaws in diffusive TPE-FCS for GL volumes are circumvented as a result of analytical treatment of the correlation function. The mathematical complexity is such that the organization of the paper revolves around the next two Sections, where the method used in the current theoretical investigation is reported with scrupulous attention to detail. The results clearly indicate that the TPE fluorescence correlation is governed by the real part of the complex error function (otherwise called Voigt function) appearing in many other spectroscopic problems.[2,27,34] On this basis, comparisons with the 3DG correlation function of eq 2 are given in the Section dedicated to the results. Last, considering the difficulties of the mathematical formalism that might be too severe for researchers that are not familiar with more advanced mathematical concepts and tools, a simplification of the calculation is shown to ease the application of the achievements of this work.

2. Theoretical Method: Comparison between 3DG and GL Distributions

Before going through the calculation, it is instructive to visualize the peculiarities of the 3DG approximation valid for a two-photon excitation. In this special case, it is straightforward to write the spatial dependence of fluorescence emission as

$$\varphi_{3DG}(\mathbf{r}) = \exp\{-4[(x^2 + y^2)/w_0^2 + z^2/z_{3DG}^2]\} \qquad (3)$$

Correspondingly, the GL distribution is

$$\varphi_{GL}(\mathbf{r}) = \frac{\exp[-4(x^2 + y^2)/w^2(z)]}{(1 + z^2/z_R^2)^2} \qquad (4)$$

where $w^2(z) = w_0^2[1 + (z/z_R)^2]$, w_0 is the laser beam waist (assumed equal for both spatial distributions), and z_{3DG} and z_R are the confocal and Rayleigh lengths, respectively. The first obvious consideration is that $\varphi_{3DG}(\mathbf{r})$ and $\varphi_{GL}(\mathbf{r})$ coincide nearby the focal plane (with $z = 0$) in virtue of the common x and y dependences. The problematic dependence is, instead, on the axial variable z that appears with different functional forms. But it must be observed that, taking $(x,y) = (0,0)$, the axial dependences in eqs 3 and 4 are similar provided that $z_{3DG} = 1.658z_R$. This is shown in Figure 1, where the 3DG and GL lobes are well-superimposed. This similarity suggests that some common features should be reflected in the correlation functions pertaining to $\varphi_{3DG}(\mathbf{r})$ and $\varphi_{GL}(\mathbf{r})$. However, the GL profile and the closest 3DG curve differ in the higher wings expected for the Lorentzian component of $\varphi_{GL}(\mathbf{r})$, and despite being small, this difference is not without consequences.

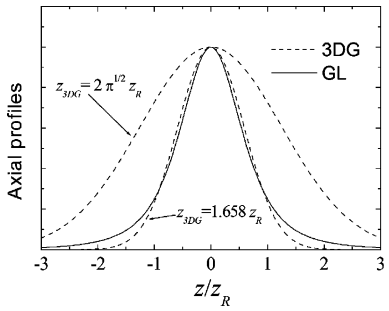

Figure 1. Axial profiles of $\varphi_{3DG}(\mathbf{r})$ and $\varphi_{GL}(\mathbf{r})$. The GL profile (continuous line) nearly coincides with the 3DG profile (dashed line) if the parameter z_{3DG} is set equal to $1.658z_R$. The broader Gaussian profile is plotted for $z_{3DG} = 2\sqrt{\pi}z_R$.

Another important comparison is between the total volumes determined by

$$V_{3DG} = \int \varphi_{3DG}(\mathbf{r})\,d\mathbf{r} = (\pi/4)^{3/2} w_0^2 z_{3DG} \qquad (5)$$

$$V_{GL} = \int \varphi_{GL}(\mathbf{r})\,d\mathbf{r} = \pi^2 w_0^2 z_R/4 \qquad (6)$$

and it is soon realized that the condition $V_{3DG} = V_{GL}$ is fulfilled only if $z_{3DG} = 2\sqrt{\pi}z_R$ corresponding to the broader Gaussian profile of Figure 1. This relationship between z_{3DG} and z_R is slightly more than two times the relationship found before by equating the widths of the axial profiles as in Figure 1. This is easily understood, because the 3DG distribution must broaden to compensate for the volume contained in the Lorentzian tails of $\varphi_{GL}(\mathbf{r})$.

The two conditions $z_{3DG} = 1.658z_R$ and $z_{3DG} = 2\sqrt{\pi}z_R$ will be very useful to orientate the discussion after the calculation of the correlation function $G_{GL}(\tau)$ for GL volumes. This calculation is laid out in the next section.

3. Theoretical Method: Calculation of the Correlation Function

Having introduced the spatial distribution $\varphi_{GL}(\mathbf{r})$ of GL volumes, it is now possible to illustrate how to get at the analytical form of the correlation function given in eq 1. To that end, we first notice that the numerator of $G(\tau)$ contains an integral with respect to six variables. In view of the arduous solution of such a multiple integral, we purposely recall that Fourier decomposition is particularly useful to simplify difficult problems set in real space. The simplification is obtained by means of the corresponding analysis within the conjugate space of momenta [here indicated with the notation $\mathbf{q} = (q_x, q_y, q_z)$]. In this respect, FCS does not make an exception, but although the application of Fourier analysis to FCS is given elsewhere,[32] we have to face that the problematic dependence on the axial

variable does not disappear. For this reason, we are forced to follow a modified version of the theory used to find the analytical correlation function for OPE set-ups.[32]

Complying with this warning means that the calculation starts with the definition of a new function $\tilde{\Phi}(q_x, q_y, z)$ taken as the Fourier transform of the radial component of $\varphi(\mathbf{r})$

$$\tilde{\Phi}(q_x, q_y, z) = \frac{1}{2\pi}\int \varphi(\mathbf{r})\exp[\mathrm{i}(q_x x + q_y y)]\,\mathrm{d}x\,\mathrm{d}y \qquad (7)$$

In this manner, the complete Fourier transform of $\varphi(\mathbf{r})$ will be

$$\Phi(\mathbf{q}) = \frac{1}{(2\pi)^{1/2}}\int \tilde{\Phi}(q_x, q_y, z)\exp(\mathrm{i}q_z z)\,\mathrm{d}z \qquad (8)$$

Now, eq 8 can be used in the known result[32]

$$\int\int \varphi(\mathbf{r})\,\psi(\mathbf{r}-\mathbf{r}', \tau)\varphi(\mathbf{r}')\,\mathrm{d}\mathbf{r}\,\mathrm{d}\mathbf{r}' = (2\pi)^{3/2}\int \Psi(\mathbf{q},\tau)|\Phi(\mathbf{q})|^2\,\mathrm{d}\mathbf{q} \qquad (9)$$

that reduces the numerator $G(\tau)$ to a multiple integral with respect to three integration variables only. The calculation on the right-hand side of eq 9 is feasible when the Fourier transform $\Psi(\mathbf{q}, \tau)$ of $\psi(\mathbf{r}, \tau)$ is not too complicated. This is true for diffusion characterized by a constant coefficient D.[33] In this instance, the Fourier transform of $\psi(\mathbf{r} - \mathbf{r}',\tau) = \langle C\rangle(4\pi D\tau)^{-3/2}\exp(-|\mathbf{r} - \mathbf{r}'|^2/4D\tau)$ is still Gaussian, $\Psi(\mathbf{q},\tau) = \langle C\rangle\exp(-D\tau q^2)/(2\pi)^{3/2}$ with $q^2 = q_x^2 + q_y^2 + q_z^2$. Using this result in eq 9 leads to

$$\int\int \varphi(\mathbf{r})\psi(\mathbf{r}-\mathbf{r}',\tau)\varphi(\mathbf{r}')\,\mathrm{d}\mathbf{r}\,\mathrm{d}\mathbf{r}' = \langle C\rangle\int \exp(-D\tau\, q^2)|\Phi(\mathbf{q})|^2\,\mathrm{d}\mathbf{q} \qquad (10)$$

and observing that $\tilde{\Phi}_{\mathrm{GL}}(q_x, q_y, z) = (w_0^2/8)\exp[-(q_x^2 + q_y^2) \times w^2(z)/16]$, the resulting calculation of eq 10 for GL volumes becomes

$$\int\int \varphi_{\mathrm{GL}}(\mathbf{r})\psi(\mathbf{r}-\mathbf{r}',\tau)\varphi_{\mathrm{GL}}(\mathbf{r}')\,\mathrm{d}\mathbf{r}\,\mathrm{d}\mathbf{r}' = \frac{\langle C\rangle\sqrt{2\pi}w_0 {z_{\mathrm{R}}}^2}{4\sqrt{t}}L_\beta(t) \qquad (11)$$

where $t = \tau/\tau_{\mathrm{D}}$, $\beta = z_{\mathrm{R}}/w_0$, and the function $L_\beta(t)$ is

$$L_\beta(t) = \pi\int \frac{1}{1+\zeta^2}\frac{1}{1+2t+\zeta^2}\{\mathrm{Re}[W(\xi_1)] - \mathrm{Re}[W(\xi_2)]/\sqrt{2(1+t)+\zeta^2}\}\,\mathrm{d}\zeta \qquad (12)$$

In eq 12, $\xi_1 = \beta\sqrt{2/t}\,(-\zeta + i)$ and $\xi_2 = \beta\sqrt{2/t}\,(-\zeta + i\sqrt{2(1+t)+\zeta^2}\,)$ are complex variables, whereas $\mathrm{Re}[W(\xi)]$ indicates the real part of the complex error function $W(\xi)$,[34] otherwise known as Voigt function, which characterizes the homogeneous (i.e., Lorentzian) and inhomogenous (i.e., Gaussian) broadening of spectroscopic line intensities.[2,27] It is then not surprising that the appearance of the Voigt function in the context of FCS is again indicative of an interplay between Lorentzian and Gaussian components (here, they belong to the spatial scales on which diffusion occurs). More importantly, in eqs 11 and 12, all the dependences are on the dimensionless variables $t = \tau/\tau_{\mathrm{D}}$, $\beta = z_{\mathrm{R}}/w_0$, $\zeta = z/z_{\mathrm{R}}$, and for this reason, $L_\beta(t)$ can be tabulated once and for all. In such a manner, $L_\beta(t)$ can be taken as an analytical function similarly to many other special functions that have integral representation and are encountered in several mathematical and physical problems.[2,27,33,34] Alternatively, $L_\beta(t)$ can be obtained in close form as linear combination of four different values of the complex error function W

$$L_\beta(t) = \pi^2\sum_{j=1}^{4} c_j(t)W(\eta_j) \qquad (13)$$

where $c_j(t)$ are time dependent coefficients and the variables η_j depend on both β and t (see the Supporting Information).

As a final step of the calculation, taking into account the normalization to the GL volume, V_{GL}, we can conclude that the TPE correlation function is

$$G_{\mathrm{GL}}(\tau) = G_{\mathrm{GL}}(0)\frac{2^{9/2}}{3\pi^{3/2}}\frac{\beta}{\sqrt{\tau/\tau_{\mathrm{D}}}}L_\beta(\tau/\tau_{\mathrm{D}}) \qquad (14)$$

with $G_{\mathrm{GL}}(0) = 3/(16N_{\mathrm{GL}})$ and $N_{\mathrm{GL}} = \langle C\rangle V_{\mathrm{GL}}$.

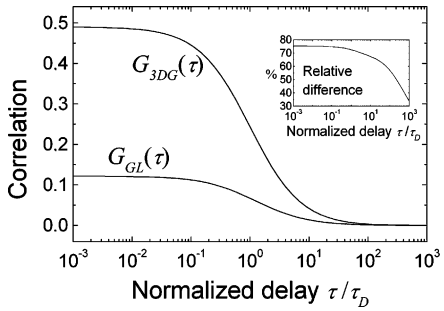

Figure 2. Correlation functions $G_{3\mathrm{DG}}(\tau)$ and $G_{\mathrm{GL}}(\tau)$ versus the normalized delay $t = \tau/\tau_D$. The 3DG approximation is applied in such a manner that it reproduces the GL axial profile of Figure 1. Optical parameters are $w_0 = 0.5$ μm, $\beta = 5$. Note that the absolute values are normalized to a common average concentration $\langle C\rangle = 1 \times 10^{15}$ molecule/L so that one molecule is guaranteed within a volume of 1 fL. In the inset, the relative difference $[G_{3\mathrm{DG}}(\tau) - G_{\mathrm{GL}}(\tau)]/G_{3\mathrm{DG}}(\tau)$ is provided.

4. Results: Comparisons between 3DG and GL Correlations

Next, we focus on the main finding of this work to compare the new correlation function $G_{\mathrm{GL}}(\tau)$ with the well-known but approximated correlation function $G_{3\mathrm{DG}}(\tau)$ given in eq 2. To achieve this aim, we suppose equal average molecular concentration $\langle C\rangle$ regardless of the model adopted to discuss the results of the current investigation. Additionally, in defining the 3DG approximation, we initially take on the Gaussian profile that best reproduces the GL profile along the axial direction, so that $z_{3\mathrm{DG}} = 1.658z_{\mathrm{R}}$ as in Figure 1. Because the similarity of the central portion of the axial profiles, this first comparison will be useful to understand the effect of the Lorentzian wings on the correlation amplitude. The decays of $G_{3\mathrm{DG}}(\tau)$ and $G_{\mathrm{GL}}(\tau)$ are shown in Figure 2 for typical values of w_0 and β (0.5 μm and 5, respectively). The most striking feature is that the amplitudes $G_{3\mathrm{DG}}(0)$ and $G_{\mathrm{GL}}(0)$ differ by about 75% (see inset), although they refer to the same average concentration $\langle C\rangle$. The difference in the amplitudes remains even though the optical parameters are varied. For example, $\beta = 2$ implies that $G_{\mathrm{GL}}(0)$ is still 75% smaller than $G_{3\mathrm{DG}}(0)$. This difference has an immediate explanation in terms of the discrepancy between the volumes (the GL volume being about 2.1 times larger than the 3DG volume).

In principle, one way to equilibrate the amplitudes is to broaden the apparent axial Gaussian profile. For instance, this

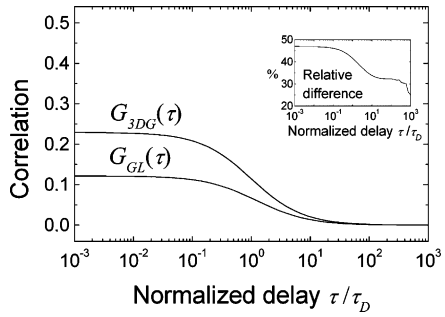

Figure 3. Correlation functions $G_{3DG}(\tau)$ and $G_{GL}(\tau)$ versus the normalized delay $t = \tau/\tau_D$. The 3DG approximation is applied in such a manner that the 3DG and GL volumes are equal (this corresponds to $z_{3DG} = 2\sqrt{\pi}\, z_{GL}$). Optical parameters are $w_0 = 0.5$ μm, $\beta = 5$. Note that the absolute values are normalized to a common average concentration $\langle C \rangle = 1 \times 10^{15}$ molecule/L so that one molecule is guaranteed within a volume of 1 fL. In the inset, the relative difference $[G_{3DG}(\tau) - G_{GL}(\tau)]/G_{3DG}(\tau)$ is provided.

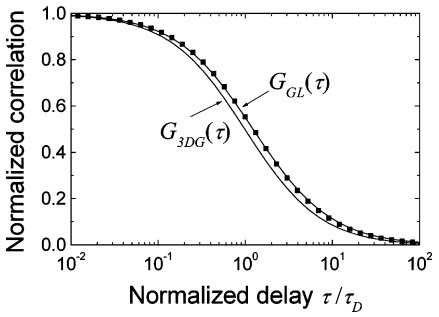

Figure 4. Normalized correlation functions. The decays of $G_{3DG}(\tau)$ and $G_{GL}(\tau)$ are indicated by the continuous lines for the parameters of Figure 2 ($w_0 = 0.5$ μm, $\beta = 5$) and $z_{3DG} = 6.69z_R$. The symbols represent instead the decay of $G_{3DG}(\tau)$ obtained as best fit to $G_{GL}(\tau)$. The fit with the 3DG approximation is identical to the decay of $G_{GL}(\tau)$ provided that the diffusion time is about 25% larger than the corresponding value for the GL approach.

results from the equality $V_{3DG} = V_{GL}$ discussed in Section 2. Under this condition, the broader axial Gaussian profile (found for $z_{3DG} = 2\sqrt{\pi}z_R \cong 3.54z_R$) is shown in Figure 1, whereas the correlation curves are reported in Figure 3. Here, for the sake of comparison, the same vertical and horizontal axes of Figure 2 have been used again. It is rather straightforward to observe that, despite this 3DG volume being larger than the 3DG volume used to generate Figure 2, the new correlation function $G_{3DG}(\tau)$ still does not agree with the theoretical GL correlation function. The relative deviation is around 45% at $\tau \ll \tau_D$ and decreases to about 25% at time delays where the correlation vanishes (see inset). In this latter time range, however, the indicated deviation is not meaningful because potential differences between the correlation functions would be lost in the experimental noise. The same conclusion is reached for comparisons where different values of β are employed.

Further increase in the Gaussian volume is of course necessary to match $G_{3DG}(0)$ and $G_{GL}(0)$. Indeed, the correlation amplitudes become identical for $z_{3DG} = 6.69z_R$, which is considerably larger than $z_{3DG} = 1.658z_R$ or $z_{3DG} = 2\sqrt{\pi}z_R$. Following a parallel reasoning, the exact match between the amplitudes could also be obtained by equating the 3DG and GL volumes calculated by means of the alternative definition found, for example, in eq 23 of ref 23. But, regardless of how the condition $G_{3DG}(0) = G_{GL}(0)$ is reached, there is a residual dissimilarity as to the time decay. This can be better analyzed if we normalize $G_{3DG}(\tau)$ and $G_{GL}(\tau)$ to their own values at vanishing times. The result is shown in Figure 4, where the decays of eqs 2 and 14 are plotted for normalized amplitudes, i.e., $G_{3DG}(0) = G_{GL}(0) = 1$. As easily noted, the two time behaviors are distinct from each other and it is obvious to conclude that a TPE-FCS measurement dealt with the 3DG approximation provides an outcome meaningfully different from the elaboration based on the GL approach here discussed. This conclusion is even more remarkable if amplitude dissimilarities (Figures 2 and 3) add to the time deviations reported in Figure 4. But this is not the end of the story. For instance, the symbols in Figure 4 mark the decay of $G_{3DG}(\tau)$ obtained as best fit to $G_{GL}(\tau)$ for a diffusion time that is about 25% larger than the corresponding value obtained under the GL approach (the increase reaches 30% for $\beta = 2$). In other words, reversing the above-mentioned conclusion, TPE-FCS measurements can be equally understood in terms of $G_{3DG}(\tau)$ or $G_{GL}(\tau)$ at the expense of noteworthy flaws arising from an unsuitable model and including extractions of incorrect optical parameters, molecular concentrations, diffusion constants, and so on.

Finally, it must be said that the whole situation depicted in Figure 4 corresponds to what is declared by some authors.[29] They noticed that TPE-FCS measurements are well replicated by either the 3DG or GL correlation function, but only the latter ensured a correct understanding of their data. Last, as a final comment, it should be mentioned that the numerical model of ref 29 was also compared to the analytical result of eq 14 and the simulations confirmed complete equivalence.

5. Results: Simplified Formulation of the GL Correlation

After the discussion about the numerical differences between the general results valid for the 3DG and GL correlation functions of TPE fluorescence of a molecule following three-dimensional Brownian diffusion, it is useful to consider another significant difference that characterizes the two theoretical approaches. This is manifest in the comparison between the easy application of eq 2 and the difficult use of the analytical result for $G_{GL}(\tau)$. Although mathematical tools are nowadays available to support researchers in the handling of complicated functions (as this work demonstrates), an attempt to simplify the analytical structure of eq 14 was made. The result is described in this Section.

The starting point is the fundamental approximation of the complex error function with purely imaginary argument (see the Supporting Information)

$$W(i\xi) \cong \frac{1}{\sqrt{\pi}\xi} \tag{15}$$

The approximation holds for large values of the real variable ξ and corresponds to the realistic conditions under which eqs 12 and 13 are calculated. The translation of eq 15 into the formalism of $L_\beta(\tau/\tau_D)$ (it does not matter which representation is chosen between the two in eqs 12 and 13) leads to the following result

$$L_\beta(\tau/\tau_D) \cong \frac{\pi^{3/2}}{2^{5/2}\beta\sqrt{\tau/\tau_D}}\left[1 + 2\frac{\tau_D}{\tau}\left(\frac{1}{\sqrt{1+\tau/\tau_D}} - 1\right)\right] \tag{16}$$

It is at once evident that the approximated result for $L_\beta(\tau/\tau_D)$ is much simpler than eq 12 or 13. In particular, the dependences on the time delay τ are made of a combination of very basic functions, namely rational and algebraic functions similar to what is seen in eq 2. With this new result in hand, we obtain a

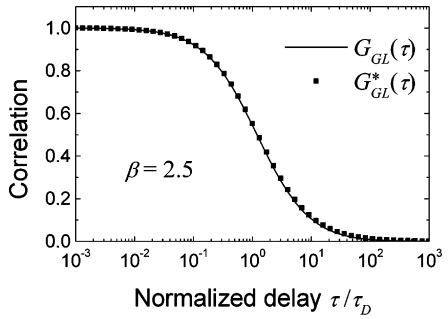

Figure 5. Normalized correlation functions $G_{GL}(\tau)$ and $G^*_{GL}(\tau)$. The approximated result of eq 17 is plotted with squares to distinguish its decay from the result of eq 14 (continuous line). The parameter β of $G_{GL}(\tau)$ is chosen equal to 2.5.

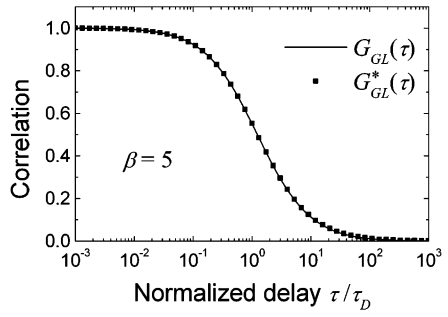

Figure 6. Normalized correlation functions $G_{GL}(\tau)$ and $G^*_{GL}(\tau)$. The approximated result of eq 17 is plotted with squares to distinguish its decay from the result of eq 14 (continuous line). The parameter β of $G_{GL}(\tau)$ is chosen equal to 5.

simplified expression of the correlation function

$$G^*_{GL}(\tau) = G_{GL}(0)\frac{4\tau_D}{3\tau}\left[1 + 2\frac{\tau_D}{\tau}\left(\frac{1}{\sqrt{1+\tau/\tau_D}} - 1\right)\right] \quad (17)$$

The star in the superscript of $G^*_{GL}(\tau)$ indicates that eq 17 is an approximated result of eq 14, and apart from the obvious simplicity of $G^*_{GL}(\tau)$ containing similar functional dependences of $G_{3DG}(\tau)$, the other relevant comparison with eq 2 is about the role of the axial width. In the classical 3DG model, adopted by most researchers, the correlation function $G_{3DG}(\tau)$ is fitted by adjusting various parameters, namely, the correlation amplitude $G_{3DG}(0)$, the diffusion time τ_D and the optical parameters w_0, z_{3DG}. Consequently, depending on the value of the axial width z_{3DG}, the ratio w_0/z_{3DG} influences the decay described by the function$G_{3DG}(\tau)$. Such parametric dependence should parallel the relationship between $G_{GL}(\tau)$ and the parameter $\beta = z_R/w_0$ defined earlier. Surprisingly, the dependence on β is absent in the simplified result of eq 17. Here, the decay is completely determined by the diffusion time τ_D and there is no need to acquire additional information on the optical parameters to generate the correlation function. This could be beneficial to fitting routines that become more robust when the number of free parameters is reduced.

To verify eq 17, a comparison with the exact result of eq 14 is shown in Figures 5 and 6. The plots of $G_{GL}(\tau)$ and $G^*_{GL}(\tau)$ are based on values of the parameter β expected to be higher than 2.5 for the experimental conditions of ref 19. Considering that $\beta = 2.42$ for the reported parameters of ref 29, the chosen range of β is realistic. Figure 5 shows the comparison for $\beta =$ 2.5 and normalized amplitudes ($G_{GL}(0) = G^*_{GL}(0) = 1$). The symbols mark the decay of $G^*_{GL}(\tau)$ that would be hardly distinguishable from $G_{GL}(\tau)$ if lines were used for both correlation curves. This constitutes a well-documented proof that the approximation leading to eq 17 is effective at reproducing the behavior of the more complicated eq 14. To strengthen this finding, another comparison is shown in Figure 6 for another typical value of $\beta = 5$. The agreement between $G_{GL}(\tau)$ and $G^*_{GL}(\tau)$ is confirmed, meaning also that the GL correlation function is practically independent from β. This last feature was further examined for larger values of the parameter. The results were identical to Figure 6, and for this reason, they are not included in this discussion.

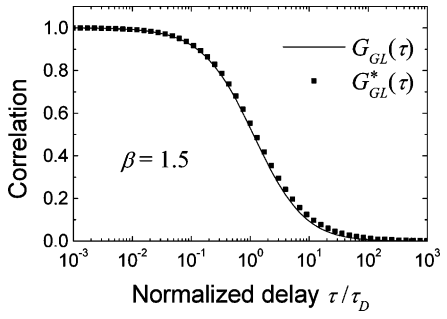

Figure 7. Normalized correlation functions $G_{GL}(\tau)$ and $G^*_{GL}(\tau)$. The approximated result of eq 17 is plotted with squares to distinguish its decay from the result of eq 14 (continuous line). The parameter β of $G_{GL}(\tau)$ is chosen equal to 1.5.

A final concern was about the equivalence of eqs 14 and 17 for a different range of the parameter ($1 < \beta < 2.5$). The consequent analysis showed that a very small difference becomes appreciable for $\beta < 2$. As an example, Figure 7 depicts the comparison for $\beta = 1.5$ corresponding to an extreme situation where for a laser wavelength of 0.78 μm, the laser beam waist should be well below 0.4 μm. In this case, even if the agreement between $G_{GL}(\tau)$ and $G^*_{GL}(\tau)$ is not so good as in Figures 5 and 6, the relative discrepancy is very small and mainly confined within the region of delays higher than the diffusion time τ_D (i.e., around $\tau = 10\tau_D$).

6. Conclusions

To sum up, the analytical calculation of the correlation function for various chemical and physical applications of diffusive TPE-FCS has been detailed for GL volumes. In view of this novelty, recognized numerical methods[29−31] become less powerful. Moreover, the general importance of GL laser beams[2,25−28] is such that the lack of analytical understanding of corresponding experimental FCS outcomes had to be filled. In this regard, the analysis shows that the complex error function, ultimately related to the physical meanings of the Voigt function, plays a crucial role. Relatively to the renowned 3DG approximation, wide discrepancies in correlation amplitudes are quantified on the order of about 75%, at the very worst. Time decays also show dissimilarities. These denote diffusion times that vary in the range of 25−30% depending on the optical parameters chosen. On the other hand, complete equivalence between the GL and 3DG models is found when one approach is adjusted to the other by means of fitting procedures. This confirms what was remarked earlier in numerical elaborations of TPE-FCS[29] and emphasizes the necessity of great care to eliminate a possible source of artifacts in this kind of experiments. Last but not least, an analytical simplification of the main result of this paper is given to facilitate the practical use of the findings about TPE-FCS of diffusion within GL volumes. The simplification reveals that the parametric dependences of the time decay are reduced to a single parameter (the diffusion time) for realistic conditions of common optical set-ups.

Acknowledgment. The support of prof. D. T. Cramb and Dr. R. F. Heuff is acknowledged for valuable comments that have been useful to deepen the matter treated in this article dedicated to L. Rivagum.

Supporting Information Available: Complete mathematical derivation of eqs 13 and 15 (PDF). This information is available free of charge via the Internet at http://pubs.acs.org.

References and Notes

(1) Magde, D.; Elson, E.; Webb, W. W. *Phys. Rev. Lett.* **1972**, *29*, 705.
(2) Demtröder, W. *Laser Spectroscopy*; Springer: Berlin, 2003.
(3) Rigler, R.; Elson, E. S., Eds. *Fluorescence Correlation Spectroscopy*; Springer-Verlag: Berlin, 2001.
(4) Maiti, S.; Haupts, U.; Webb, W. W. *Proc. Natl. Acad. Sci. U.S.A.* **1997**, *94*, 11753.
(5) Schwille, P.; Bieschke, J.; Oehlenschläger, F. *Biophys. Chem.* **1997**, *66*, 211.
(6) Hess, S. T.; Huang, S.; Heikal, A. A.; Webb, W. W. *Biochemistry* **2002**, *41*, 697.
(7) Krichevsky, O.; Bonnet, G. *Rep. Prog. Phys.* **2002**, *65*, 251.
(8) Medina, M. A.; Schwille, P. *BioEssays* **2002**, *24*, 758.
(9) Alexandrakis, G.; Brown, E. B.; Tong, T. T.; McKee, T. D.; Campbell, R. B.; Boucher, Y.; Jain, R. K. *Nat. Med.* **2004**, *10*, 203.
(10) Lippincott-Schwartz, J.; Snapp, E.; Kenworthy, A. *Nat. Rev. Mol. Cell Biol.* **2001**, *2*, 444.
(11) Kogure, T.; Karasawa, S.; Araki, T.; Saito, K.; Kinjo, M.; Miyawaki, A. *Nature Biotechol.* **2006**, *24*, 577.
(12) Schwille, P.; Haupts, U.; Maiti, S.; Webb, W. W. *Biophys. J.* **1999**, *77*, 2251.
(13) Bacia, K.; Kim, S. A.; Schwille, P. *Nat. Methods* **2006**, *3*, 83.
(14) Pitschke, M.; Prior, R.; Haupt, M.; Riesner, D. *Nat. Med.* **1998**, *4*, 832.
(15) Heinze, K. G.; Koltermann, A.; Schwille, P. *Proc. Natl. Acad. Sci. U.S.A.* **2000**, *97*, 10377.
(16) Mukhopadhyay, A.; Bae, S. C.; Zhao, J.; Granik, S. *Phys. Rev. Lett.* **2004**, *93*, 236105.
(17) Larson, D. R.; Zipfel, W. R.; Williams, R. M.; Clark, S. W.; Bruchez, M. P.; Wise, F. W.; Webb, W. W. *Science* **2003**, *300*, 1434.
(18) Heuff, R. F.; Swift, J. L.; Cramb, D. T. *Phys. Chem. Chem. Phys.* **2007**, *9*, 1870.
(19) Heuff, R. F.; Marrocco, M.; Cramb, D. T. *J. Phys. Chem. C* **2007**, *111*, 18942.
(20) Lumma, D.; Keller, S.; Vilgis, T.; Rädler, J. O. *Phys. Rev. Lett.* **2003**, *90*, 218301.
(21) Dittrich, P. S.; Schwille, P. *Appl. Phys. B* **2001**, *73*, 829.
(22) Aragón, S. R.; Pecora, R. *J. Chem. Phys.* **1976**, *64*, 1791.
(23) Hess, S. T.; Webb, W. W. *Biophys. J.* **2002**, *83*, 2300.
(24) Zipfel, W. R.; Williams, R. M.; Webb, W. W. *Nat. Biotechnol.* **2003**, *21*, 1369.
(25) Qian, H.; Elson, E. L. *Appl. Opt.* **1991**, *30*, 1185.
(26) Webb, R. H. *Rep. Prog. Phys.* **1996**, *59*, 427.
(27) Yariv, A. *Quantum Electronics;* John Wiley & Sons: New York, 1989.
(28) Self, S. A. *Appl. Opt.* **1983**, *22*, 658.
(29) Berland, K. M.; So, P. T. C.; Gratton, E. *Biophys. J.* **1995**, *68*, 694.
(30) Goyan, R.; Paul, R.; Cramb, D. T. *J. Phys. Chem. B* **2001**, *105*, 2322.
(31) Unruh, J. R.; Price, E. S.; Molla, R. G.; Rongqing, H.; Johnson, C. K. *Microsc. Res. Tech.* **2006**, *69*, 891.
(32) Marrocco, M. *Chem. Phys. Lett.* **2007**, *449*, 227.
(33) Cranck, J. *The Mathematics of Diffusion*; Oxford University Press: Oxford, U.K., 1993.
(34) Abramowitz, M.; Stegun, I. A. *Handbook of Mathematical Functions*; Dover: New York, 1974.